Supporting Information

Vertically aligned boron-doped diamond nanostructures as highly efficient electrodes for electrochemical supercapacitors

Shradha Suman,[ab] Dhananjay Kumar Sharma,[c] Ondrej Szabo,[c] Benadict Rakesh,[ab] Umapathi Balaji,[ab] Marian Marton,[d] Marian Vojs,[d] Andrej Vincze,[e] Soumya Prakash Dutta,[ab] Debidutta Debasish,[ab] Ramasamy Sakthivel,[ab] Kamatchi Jothiramalingam Sankaran,[*ab] and Alexander Kromka[*c]

[a]*CSIR-Institute of Minerals and Materials Technology, Bhubaneswar 751013, India. E-mail: kjsankaran@immt.res.in*

[b]*Academy of Scientific and Innovative Research (AcSIR), Ghaziabad 201002, India.*

[c]*Institute of Physics of the Czech Academy of Sciences, 16200 Prague, Czech Republic. E-mail: kromka@fzu.cz*

[d]*Institute of Electronics and Photonics, Slovak University of Technology, 81219 Bratislava, Slovakia.*

[e]*International Laser Centre, Slovak Centre of Scientific and Technical Information (SCSTI), 84104 Bratislava, Slovak Republic*

Mechanism of boron-doping into diamond lattice:

The boron doping in diamond films is done at the synthesis step. The precursor gas contains the boron to be doped in the diamond lattice. For the BDD film growth, Trimethyl borate (TMBT) was used as the carbon, boron and oxygen source. The flow rate of TMBT for the formation of the pristine sample is optimised for the two morphological BDD.[S1] TMBT under microwave plasma conditions gives rise to a number of plasma-activated reactions within the processing chamber.[S2] A set of chemical reactions have been proposed to be occurring during the plasma process, which implies the generation of free active C and B atoms:

$$B(CH_3O)_3 + H_2 \rightarrow 2CH_4 + H_3BO_3 + C$$

$$H_3BO_3 \rightarrow HBO_2 + H_2O$$

$$HBO_2 + 2H_2O \rightarrow B(OH)_4 + 0.5H_2$$

$$B(OH)_4 + 2H_2 \rightarrow B + 4H_2O$$

$$CH_4 + H^* \rightarrow CH_3 + H_2$$

The presence of methyl radical in the plasma promotes the diamond growth while the free active boron atom dopes the diamond resulting in BDD.[1,2]

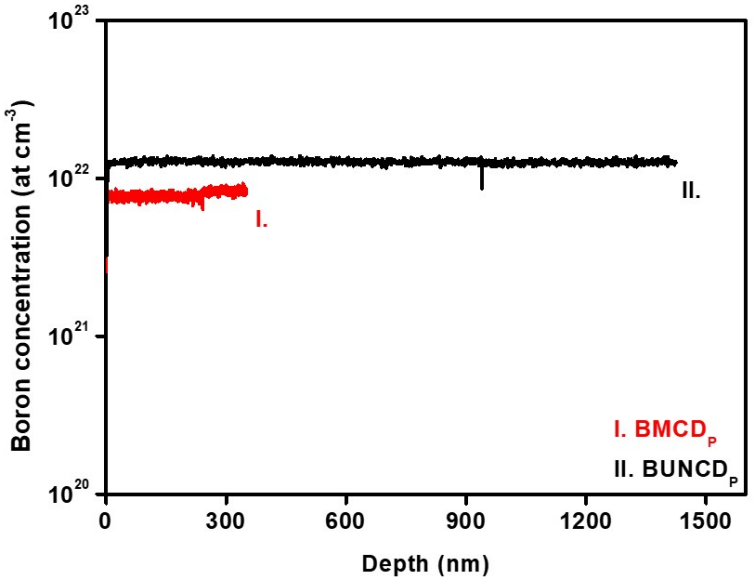

Fig. S1. ToF-SIMS positive ion depth profiles for I. BMCD$_P$ and II. BUNCD$_P$.

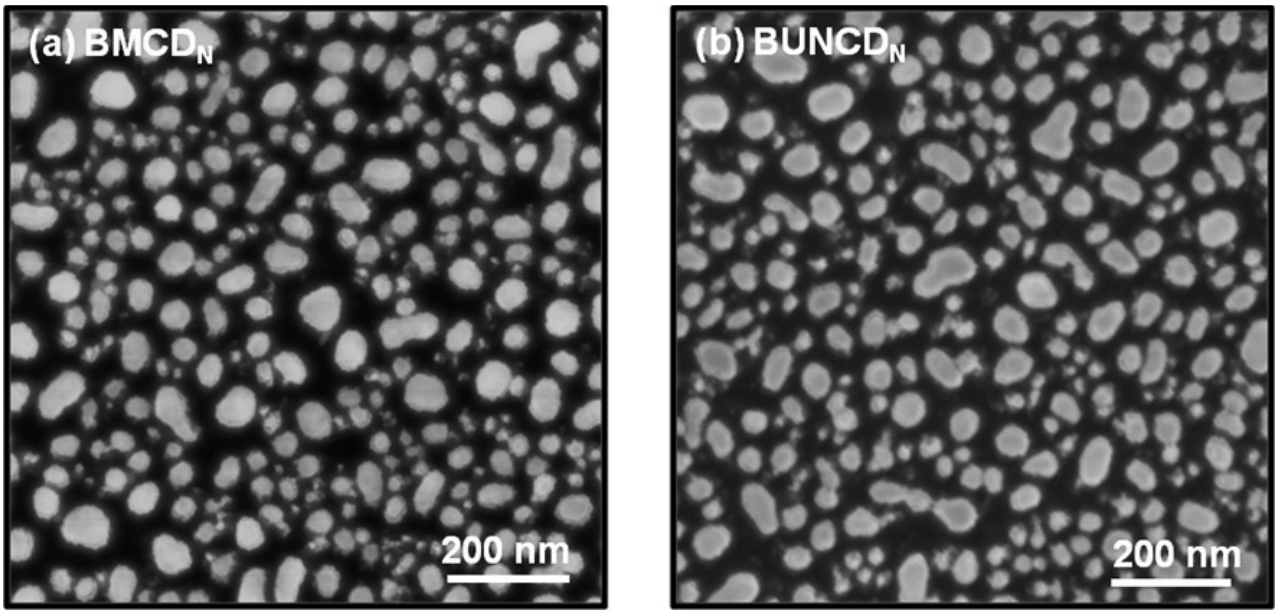

Fig. S2. The top view FESEM images of (a) $BMCD_N$, and (b) $BUNCD_N$.

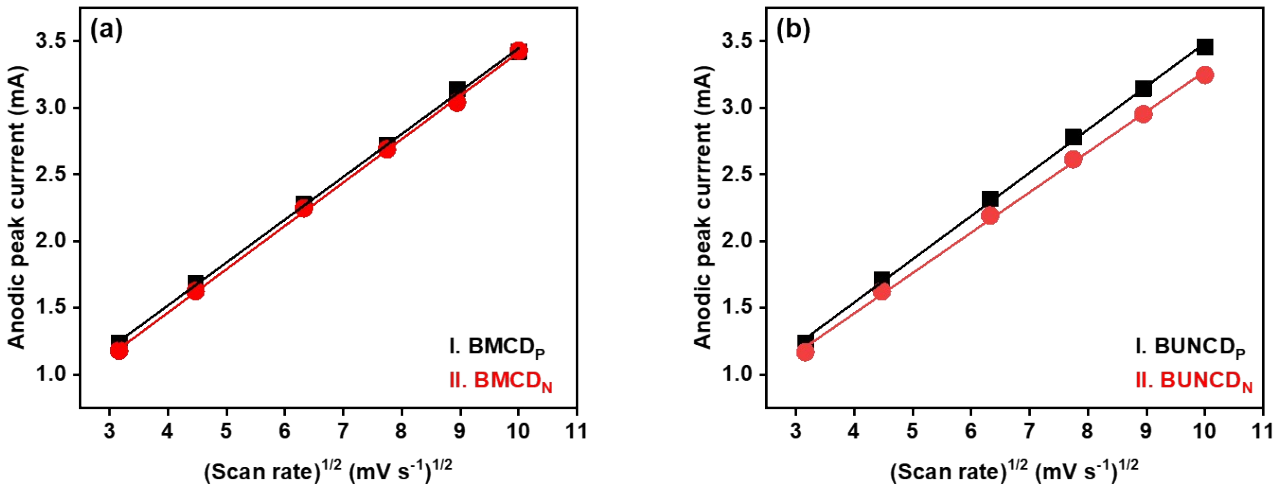

Fig. S3. The comparison of anodic peak current versus square root of scan rate in the 0.05M $Fe(CN)_6^{3-/4-}$ in 1M Na_2SO_4 electrolyte of (a) BMCD series: I. $BMCD_P$, and II. $BMCD_N$, (b) BUNCD series: I. $BUNCD_P$, and II. $BUNCD_N$.

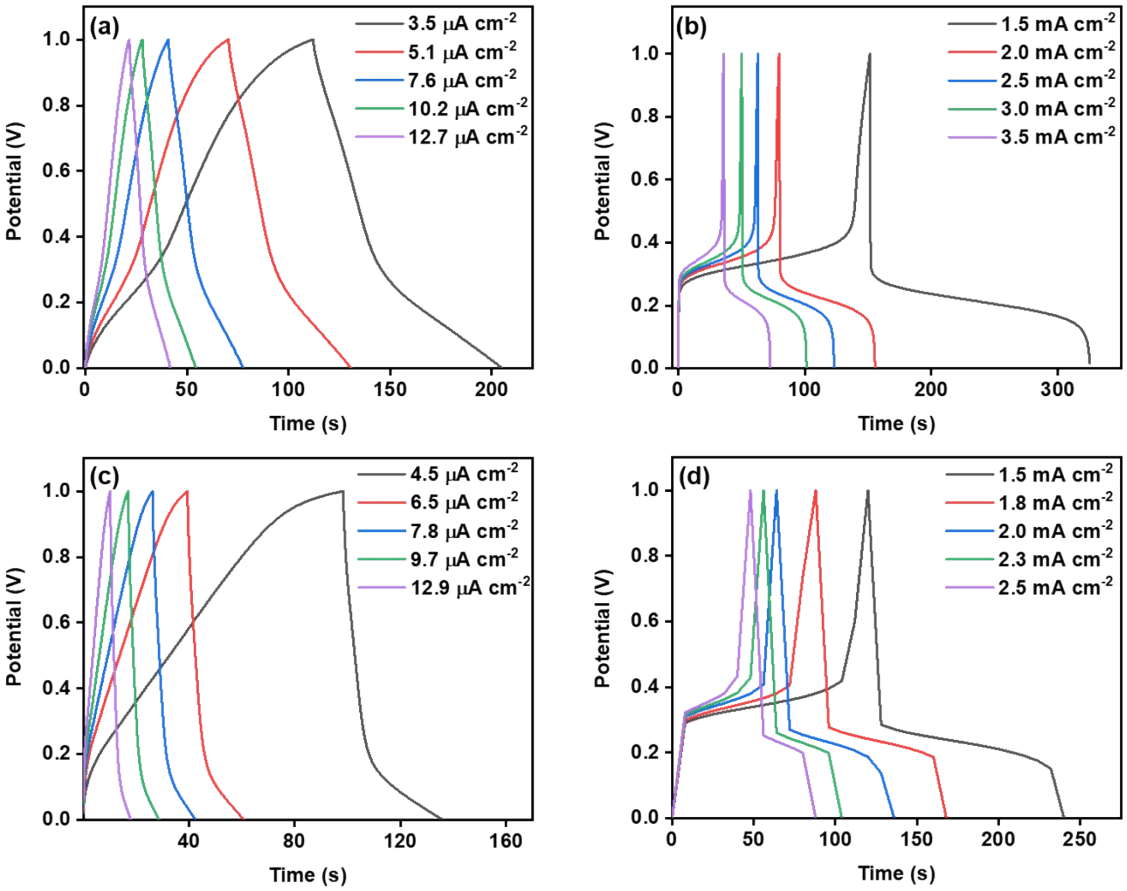

Fig. S4. The galvanostatic charging discharging measurement in 1M Na_2SO_4 for (a) $BMCD_P$ and (c) $BUNCD_P$, and in the 0.05M $Fe(CN)_6^{3-/4-}$ in 1M Na_2SO_4 electrolyte of (b) $BMCD_P$ and (d) $BUNCD_P$.

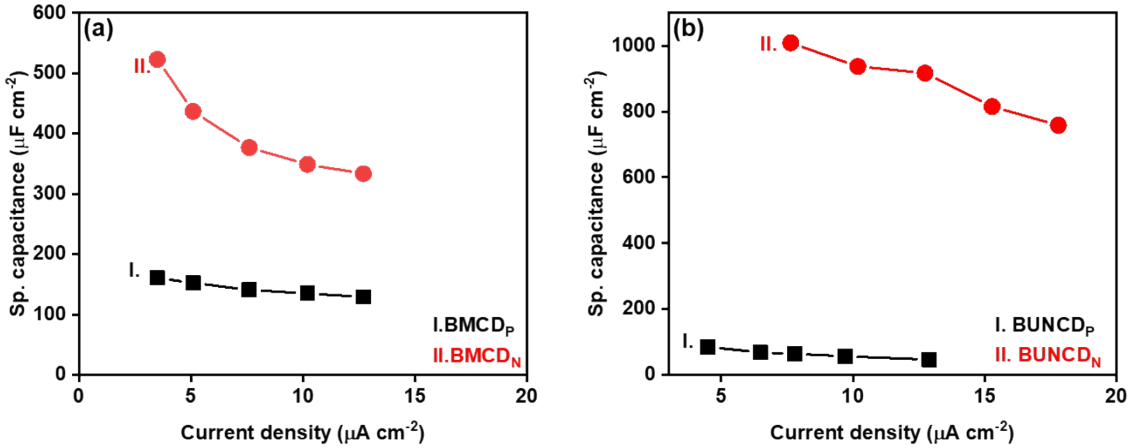

Fig. S5. The comparison of specific capacitance calculated from the GCD measurements in 1M Na_2SO_4 of (a) BMCD series: I. $BMCD_P$ and II. $BMCD_N$, (b) BUNCD series: I. $BUNCD_P$ and II. $BUNCD_N$.

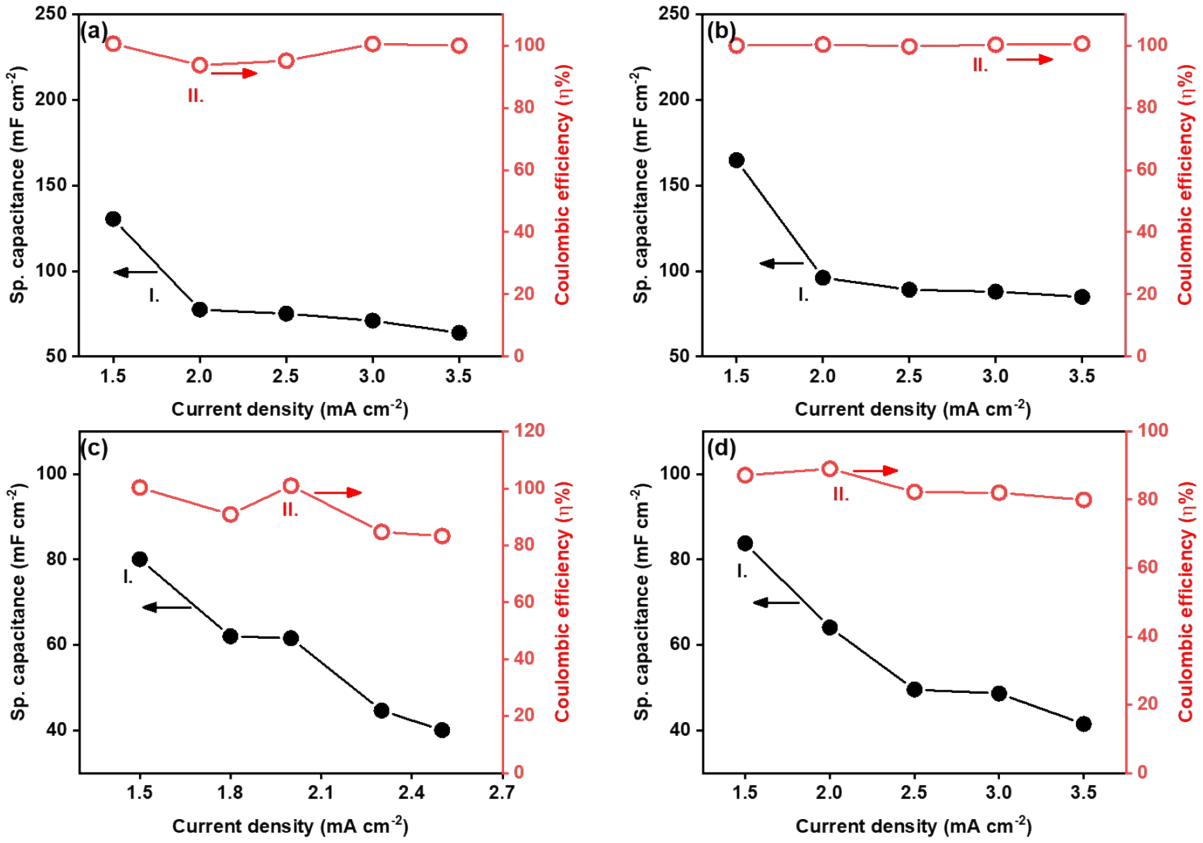

Fig. S6. The specific capacitance and coulombic efficiency plot measured in 0.05M $Fe(CN)_6^{3-/4-}$ in 1M Na_2SO_4 electrolyte of (a) $BMCD_P$, and (b) $BMCD_N$, (c) $BUNCD_P$, and (d) $BUNCD_N$.

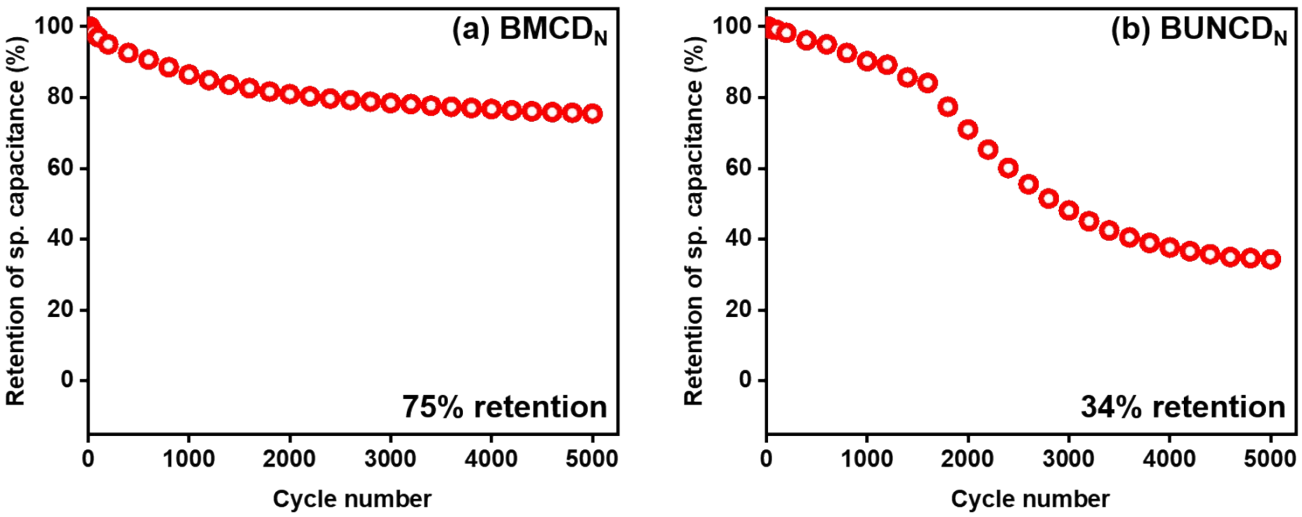

Fig. S7. Retention of specific capacitance in 0.05M $[Fe(CN)_6]^{3-/4-}$ in 1M Na_2SO_4 electrolyte for (a) $BMCD_N$ and (b) $BUNCD_N$ sample.

The specific capacity retention of the nanostructured samples in the redox-active electrolyte is shown in Fig. S7 . After 5000 cycles $BMCD_N$ and $BUNCD_N$ show 75% and 36% of retention of specific capacitance, respectively.

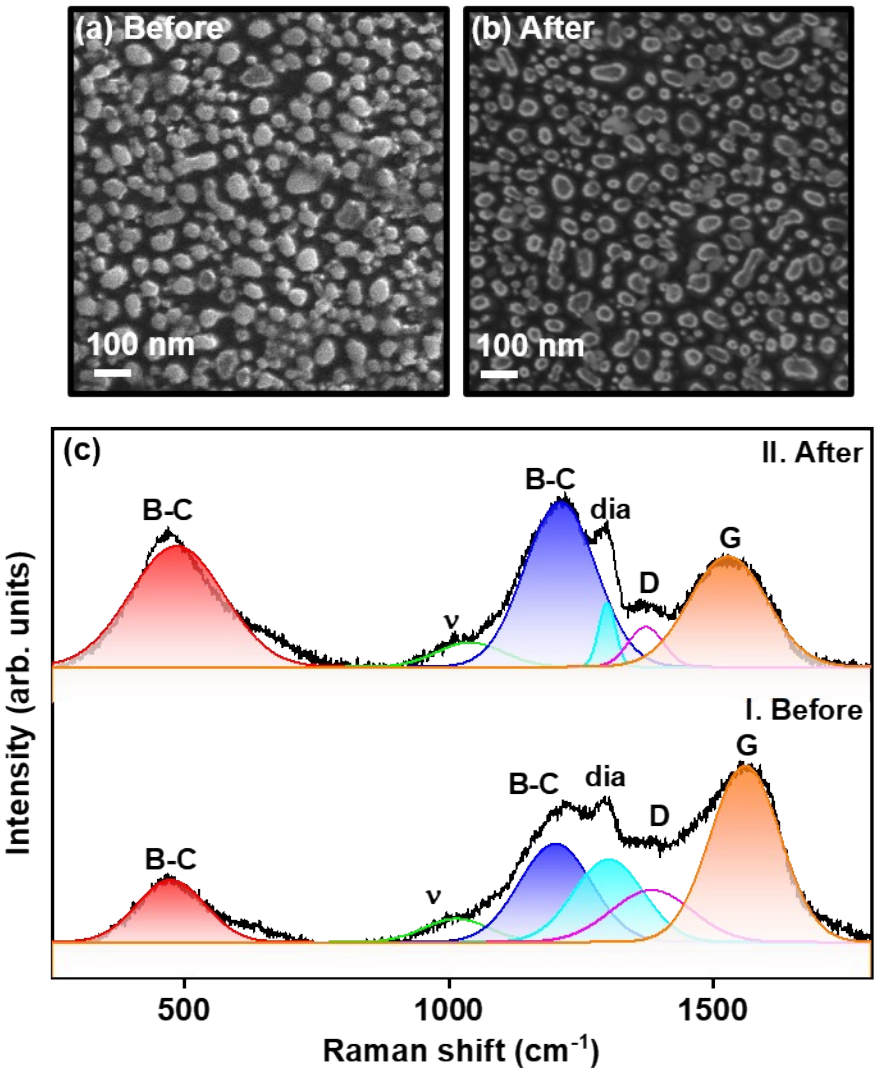

Fig. S8. FESEM micrographs of $BMCD_N$ (a) before and (b) after 5000 cycles of charging-discharging in 1M Na_2SO_4 and (c) comparison of Raman spectra I. before and II. after the lifecycle test in 1M Na_2SO_4.

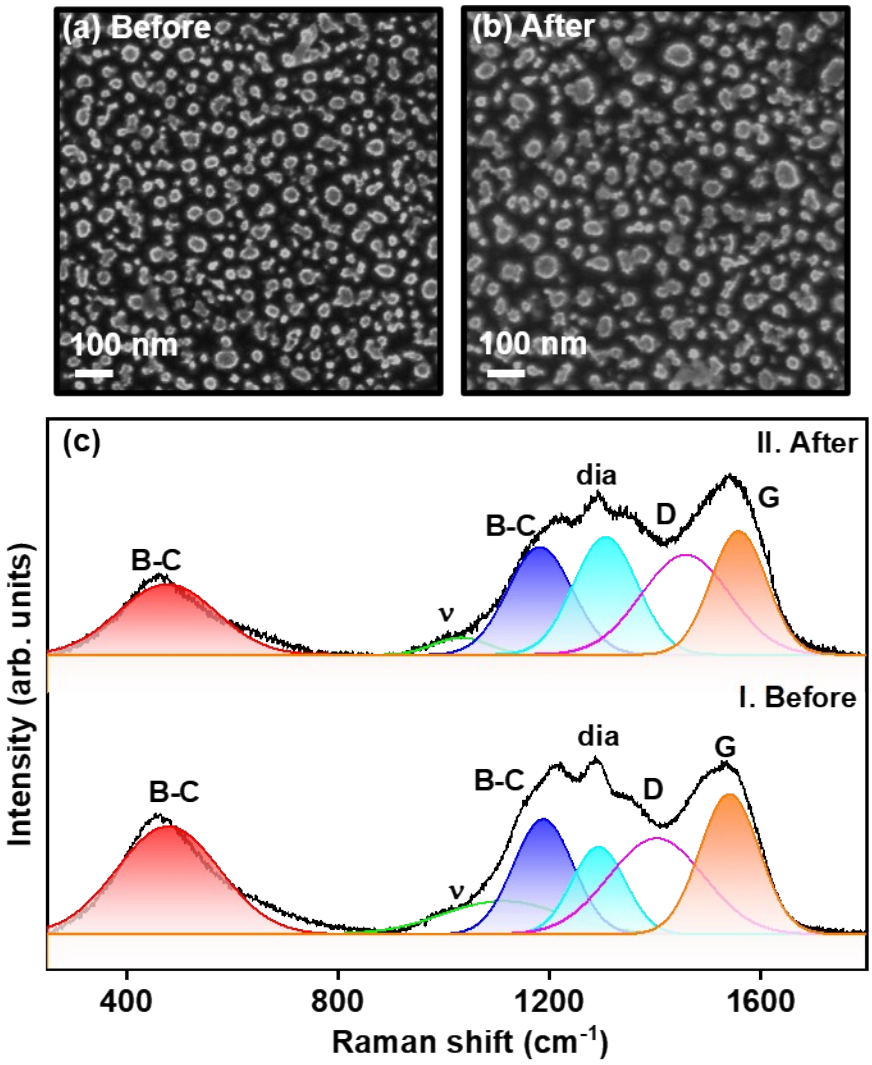

Fig. S9. FESEM micrographs of $BUNCD_N$ (a) before and (b) after 5000 cycles of charging-discharging in 1M Na_2SO_4 and (c) comparison of Raman spectra I. before and II. after the lifecycle test in 1M Na_2SO_4.

Table S1: **A comparison of characteristic Raman peaks of $BMCD_N$ and $BUNCD_N$ electrodes.**

	A_{dia}/ A_G	I_G/I_{dia}	I_D /I_G
$BMCD_N$			
Before	0.0389	1.8588	0.3974
After	0.1105	1.4869	0.4821
$BUNCD_N$			
Before	0.5660	1.6021	0.6819
After	1.0879	1.0471	0.8161

References:

S1. M. Marton, M. Vojs, P. Michniak, M. Behúl, V. Rehacek, M. Pifko, Š. Stehlík, and A. Kromka, *Diam Relat Mater* **126**, 109111 (2022).

S2. N. Makuch, P. Dziarski, M. Kulka, Coatings, **10**, 564 (2020).